

Barycentric coordinates for convex sets

Joe Warren¹, Scott Schaefer¹, Anil N. Hirani² and Mathieu Desbrun³

¹Rice University
6100 Main St.
Houston, TX 77005

²Caltech
1200 E. California Boulevard
Pasadena, CA 91125

³University of Southern California
3737 Watt Way, PHE 434
Los Angeles, CA 90089

Abstract

Barycentric coordinates are one of the most basic mathematical tools in graphics, as well as in many computational sciences. Although the formulas for simplices (triangles, tetrahedra and so on) are widely known and routinely used, there has been no satisfactory extension of these to arbitrary convex polytopes despite a plethora of potential applications. In this paper, we propose a simple, computationally convenient formula of a canonical form of barycentric coordinates. These functions are rational, smooth and of low degree. Next, we extend the formulas for convex polytopes to smooth, convex functions. Finally, we present an application of barycentric coordinates to free-form deformation.

1 Introduction

Introduced by Möbius in 1827 as *mass points* to define a coordinate-free geometry, barycentric coordinates over simplices are a very common tool in all sorts of computation. In addition to their coordinate-free expressions, barycentric coordinates are extremely helpful for interpolating discrete scalar fields, vector fields or arbitrary multidimensional fields over irregular tessellations: they naturally interpolate values at vertices to the whole space via multilinear interpolation. Their use over triangles or tetrahedra is routine in graphics, be it in hardware or software, as well as in many other applied fields such as in computational physics and mechanics via the finite element method.

The graphics community has made extensive use of barycentric coordinates since the beginning of the field. In early work barycentric coordinates were mostly for triangles, with applications such as polygon rasterization, texture mapping, ray-triangle intersection in raytracing, spline patches, interpolation etc. More recently, barycentric coordinates for tetrahedra have been used for interpolation of 3D fields for volume rendering or isosurface extraction, as well as for simulation purposes since they define convenient linear basis functions over simplices. Data in even higher dimensions, such as for lightfield applications, also require appropriate interpolation between discrete samples.

A natural question arises when interpolation is needed over more complex shapes, such as polygons or polytopes: can we extend this notion of barycentric coordinates to arbitrary polytopes? The common way to deal with irregular polygons in 2D, or general polyhedra in 3D, is to triangulate them first, and apply barycentric coordinates on each simplex. However this solution is unacceptable for many applications: the results depend on the choice of triangulation, and contain unnecessary visual artifacts (due to only C^0 continuity).

Therefore, there is a need for defining a notion of *generalized* barycentric coordinates, that would be valid for arbitrary polytopes, and would match the conventional coordinates for simplices. Such a generalization must combine *simplicity* and *computational convenience* to be a truly useful tool. The main contribution of this paper

is to provide such an extension in arbitrary dimension, along with an intuitive geometric interpretation of its validity.

1.1 Definitions

Given a convex polygon (or polyhedron) P with vertices v_i , our problem is to construct one coordinate function $b_i[x]$ per vertex v_i of P . These functions are *barycentric coordinates* with respect to P if they satisfy three properties. First, the coordinate functions are *non-negative* on P ,

$$b_i[x] \geq 0,$$

for all $x \in P$. Second, the functions form a *partition of unity*

$$\sum_i b_i[x] = 1,$$

for all x . Finally, the functions act as coordinates in that, given a value of x , weighting each vertex v_i by $b_i[x]$ returns back x .

$$\sum_i v_i b_i[x] = x. \quad (1)$$

This final property is also sometimes referred to as *linear precision* since the coordinate functions can reproduce the linear function x .

If P is the convex hull of $d + 1$ affinely independent points v_0, v_1, \dots, v_d , P is a *simplex*. For simplices, these three conditions are sufficiently restrictive that there exists only one set of barycentric coordinate functions $b_i[x]$. These functions are linear and can be computed as the ratio of two volumes

$$b_i[x] = \frac{\text{Vol}[v_0, \dots, v_{j-1}, x, v_{j+1}, \dots, v_d]}{\text{Vol}[v_0, \dots, v_{j-1}, v_j, v_{j+1}, \dots, v_d]}$$

where Vol measures the volume of the simplex defined by the $d + 1$ points. Given values f_i at the vertices v_i of the simplex P , we can construct a linear function $f[x]$ that interpolates these values (i.e.; satisfies $f[v_i] = f_i$) via the equation

$$f[x] = \sum_i f_i b_i[x] \quad (2)$$

Note that if P is not a simplex, the three properties do not uniquely determine the barycentric coordinate functions $b_i[x]$. In particular, many types of barycentric coordinates are now possible. However, as long as the barycentric coordinate functions satisfy the three fundamental properties, the coordinate function can still be used to form an interpolant as done in equation 2.

Our goal in this paper is to construct a particularly simple and elegant set of barycentric coordinates for convex sets. To guide our search, we argue that in addition to their three defining properties, barycentric coordinate functions should satisfy the following four natural auxiliary properties

Smoothness The coordinate functions should be smooth in x . This property ensures that any interpolant build with the coordinates is smooth.

Simplicity The coordinate functions should be simple to evaluate. In our case, we restrict our search to coordinate functions that are rational in x .

Tensor product If the polytope P is the tensor product of two lower dimensional polytopes, the coordinate functions $b_i[x]$ should be the tensor product of the barycentric coordinates for these lower dimensional polytopes. For instance, the barycentric coordinates for a rectangle should be bilinear coordinates, as widely used in numerical computations on regular grids.

Face restriction Restricting barycentric coordinates for a polyhedron to one of its facets should yield the same coordinates as defining the coordinates directly on the facet. For example, barycentric coordinates over a square pyramid should be bilinear on the square face of the pyramid.

1.2 Previous work

Most of the previous work on barycentric coordinates focuses on convex polygons in the plane. For the case of *regular* polygons, Loop and De Rose [Loop and DeRose 1989], Kuriyama [Kuriyama 1993] and Lodha [Lodha 1993] propose a simple construction that satisfy all of the properties above. Their expressions nicely extend the well known area-based formula for barycentric coordinates in a triangle. Unfortunately, none of the proposed constructions have linear precision when applied to irregular polygons. However, Loop and DeRose [Loop and DeRose 1989] note in their conclusion that barycentric coordinates defined over arbitrary convex polygons would open many extensions to their work.

Pinkall and Polthier [Pinkall and Polthier 1993], and later Eck et al. [Eck et al. 1995], present a conformal parameterization for triangulated surfaces that actually provides a natural extension of barycentric coordinates to arbitrary polygons. However, the weights they define can be negative even when the polygon is convex [Meyer et al. 2002], which can be problematic for interpolation applications.

Floater [Floater 1997; Floater 1998] gives an algorithmic construction coordinates over star-shaped regions in 2D. However, this construction suffers from the drawback that the result coordinate functions are not smooth within the polygon. In recent work Floater and colleagues [Floater 2002; Floater et al. 2003] also present smooth coordinates for non-convex polygons based on the mean value theorem. However this family of methods do not satisfy the tensor product property. In particular, mean value coordinates are not bilinear on rectangles. Sibson [Sibson 1981] proposes a natural neighbor interpolant based on Voronoi diagram that yields coordinate functions that are non-negative and have linear precision; note also that Gotsman and colleagues proposed a minimization-driven barycentric coordinates [Gotsman and Surahhsky 2001]. Again, the drawback with these constructions is that the coordinate functions are not smooth.

Our construction is the culmination of a line of research starting with Wachspress [Wachspress 1975] and Meyer et al. [Meyer et al. 2002] where rational barycentric coordinate functions for convex polygons are constructed and continuing through Warren [Warren 1996] where a general, but abstract, construction is given for barycentric coordinates over arbitrary polytopes. Warren [Warren 2002] has recently shown that this barycentric construction yields rational coordinates of minimal degree.

Contributions Our contribution in this paper is to give a direct, explicit construction (including pseudo-code for the 3D case) for

barycentric coordinates over an arbitrary convex polytope. Our coordinates are rational functions of minimum possible degree that also satisfy the tensor product property and the face restriction properties. Due to its simplicity, this construction can be extended to smooth convex sets using geometric quantities such as tangent planes and Gaussian curvature. To conclude, we demonstrate a simple application of the resulting coordinates in defining a deformation of a smooth convex region.

2 Barycentric coordinates for convex polytopes

Given a d -dimensional vector $x = (x_1, \dots, x_d)$, we define a convex region P as the solution to the matrix inequality $Nx \leq c$ where N is a $m \times d$ matrix and c is a column vector of length m . Without loss of generality, we assume that N has minimal size. If P is bounded, P is a *convex polytope*; in particular, when $d = 2$, P is a *convex polygon*, and when $d = 3$, P is a *convex polyhedra*

Instead of assigning an integer index to each vertex of P , we instead assign an index j to each facet of P corresponding to the equation $N_j x = c_j$ where N_j is the j -th row of N . Now, each vertex of P is assigned an index set σ that corresponds to the indices of those facets of P that contain v . Specifically, we index v_σ by the maximal set of integers $\sigma \subseteq \{1, \dots, m\}$ such that $N_j v_\sigma = c_j$ for all $j \in \sigma$.

2.1 The general formula for convex polytopes

A vertex v_σ is *simple* if v_σ is the intersection of d half-spaces, i.e; σ exactly contains d indices. A polytope P is simple if every vertex of P is simple. Note that convex polygons are always simple while only a subset of convex polyhedra are simple. For example, tetrahedra, cubes and triangular prisms are simple while square pyramids and octahedra are not. Drawing from Warren [Warren 1996], the barycentric coordinates for simple polytopes have the following form. Let N_σ correspond to the $d \times d$ submatrix of N whose rows are the vectors N_j where $j \in \sigma$. We define a *weight function* $w_\sigma[x]$ for every vertex v_σ of the form

$$w_\sigma[x] = \frac{|\text{Det}[N_\sigma]|}{n_\sigma[x]} \quad (3)$$

where $n_\sigma[x]$ is the product of the d linear functions $c_j - N_j x$ where $j \in \sigma$. Note that this weight function depends only on the facets incident on v_σ . In particular, the determinant in the numerator corresponds to the volume of the parallelepiped spanned by the outward normal vectors N_j associated with the facets incident on v_σ , while the denominator is the product of the distances between x and the d facets adjacent to v_σ .

Finally, the barycentric coordinate function $b_\sigma[x]$ is formed by dividing each weight function $w_\sigma[x]$ by the sum of all weight functions taken over P .

At this point, we make several quick observations concerning the structure of these functions $b_\sigma[x]$. First, these function are non-negative on P due to the fact that the weight functions $w_\sigma[x]$ are, by construction, non-negative on P . Second, these functions trivially sum to one by construction. Third, these functions have linear precision. Proving that the functions $b_\sigma[x]$ have linear precision reduces to showing that the associated weight functions $w_\sigma[x]$ satisfy the equation

$$\sum_{v_\sigma \in P} (v_\sigma - x) w_\sigma[x] = 0. \quad (4)$$

The attached appendix proves that the weight functions defined by equation 3 satisfy this equation.

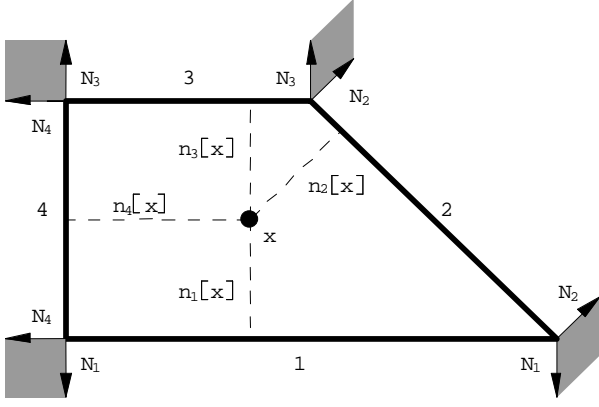


Figure 1: The example trapezoid with bounding halfplanes (labeled 1-4), normals (N_1 - N_4), and distances ($n_i[x]$). The areas of the shaded parallelograms formed by the normals correspond to the quantity $|\text{Det}[N_\sigma]|$.

Given that the functions $b_\sigma[x]$ are non-negative, form a partition of unity and have linear precision, these functions define barycentric coordinates over P . Moreover, we also claim that these barycentric coordinates are smooth, reproduce tensor product coordinates and satisfy the face restriction property. The key observation is to note that, if P is polytope with m facets in d dimensions, $b_\sigma[x]$ is a rational function of degree $m-d$. Thus, these coordinate functions are smooth and simple to evaluate. As for the remaining two properties (tensor product and face restriction), Warren [Warren 2002] shows that there exists only one set of rational barycentric coordinate functions of degree $m-d$ for a polytope with m facets in d dimensions. Moreover, this set of coordinate functions reproduces tensor product coordinates and satisfies the face restriction property. Since the proposed coordinates are barycentric and of degree $m-d$, they must satisfy these two properties.

2.2 Examples

To illustrate the concrete nature of equation 3, we next consider several examples in various dimensions.

Line segments

In the univariate case, the vector x has the form (x_1) . We next construct barycentric coordinate for interval $[a, b]$. This interval is defined as the intersection of two half-intervals satisfying

$$\begin{pmatrix} -1 \\ 1 \end{pmatrix} x_1 \leq \begin{pmatrix} -a \\ b \end{pmatrix}.$$

By construction, the corresponding weight functions are $(w_1[x_1], w_2[x_2]) = (\frac{1}{x_1-a}, \frac{1}{b-x_1})$. Normalizing these weight functions to sum to one yields the functions for linear interpolation on the interval $[a, b]$,

$$\begin{aligned} b_1[x_1] &= \frac{b-x_1}{b-a}, \\ b_2[x_1] &= \frac{x_1-a}{b-a}. \end{aligned}$$

Convex polygons

In the plane, a convex m -gon can be written as the intersection of m -halfplanes with each halfplane defining an edge of the m -gon. If we index these halfplanes (and edges) of the convex m -gon in clockwise order, each vertex of the m -gon can be expressed as the

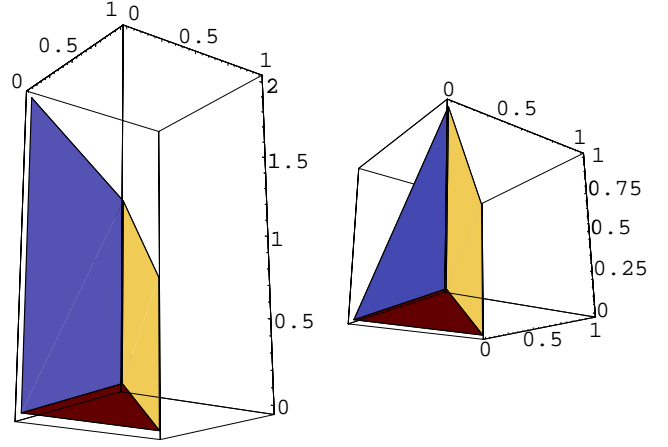


Figure 2: A triangular prism (left) and a square pyramid (right).

intersection of consecutive edges. For example, consider the trapezoid of figure 1 defined by the four halfplanes,

$$\begin{pmatrix} -1 & 0 \\ 0 & -1 \\ 1 & 1 \\ 0 & 1 \end{pmatrix} \begin{pmatrix} x_1 \\ x_2 \end{pmatrix} \leq \begin{pmatrix} 0 \\ 0 \\ 2 \\ 1 \end{pmatrix}$$

The trapezoid enclosed by these halfplanes contains the vertices $\{v_{\{1,2\}}, v_{\{2,3\}}, v_{\{3,4\}}, v_{\{1,4\}}\}$, which correspond to the points $\{(2, 0), (1, 1), (0, 1), (0, 0)\}$, respectively.

Applying formula 3 yields weight functions $w_\sigma[x]$ of the form

$$\begin{aligned} w_{\{1,2\}}[x_1, x_2] &= \frac{1}{x_1 x_2}, \\ w_{\{2,3\}}[x_1, x_2] &= \frac{1}{(2-x_1-x_2)x_2}, \\ w_{\{3,4\}}[x_1, x_2] &= \frac{1}{(1-x_2)(2-x_1-x_2)}, \\ w_{\{1,4\}}[x_1, x_2] &= \frac{1}{x_1(1-x_2)}. \end{aligned}$$

The corresponding barycentric coordinate functions follow by dividing each of these weight function by their sums. Notice that those coordinates exactly match the ones introduced in [Meyer et al. 2002] for convex polygons (simple trigonometry shows equivalence).

Convex polyhedra

In 2D, all polygons are simple; that is every vertex is the intersection of two edges. In three dimensions, a vertex of a polyhedron can lie on more than three faces. For the sake of simplicity, we begin by considering barycentric coordinates for a triangular prism. In this case, equation 3 is applicable without modification. For example, consider a triangular prism as the intersection of 5 half-spaces as shown in left part of figure 2.

$$\begin{pmatrix} -1 & 0 & 0 \\ 0 & -1 & 0 \\ 1 & 1 & 0 \\ 0 & 0 & -1 \\ 1 & 1 & 1 \end{pmatrix} \begin{pmatrix} x_1 \\ x_2 \\ x_3 \end{pmatrix} \leq \begin{pmatrix} 0 \\ 0 \\ 1 \\ 0 \\ 2 \end{pmatrix}.$$

These half-space intersect in a polyhedron with six simple vertices indexed as

$$v_{\{1,2,4\}}, v_{\{1,3,4\}}, v_{\{2,3,4\}}, v_{\{1,2,5\}}, v_{\{1,3,5\}}, v_{\{2,3,5\}}$$

with corresponding positions

$$(0, 0, 0), (0, 1, 0), (1, 0, 0), (0, 0, 2), (0, 1, 1), (1, 0, 1).$$

Applying formula 3, the corresponding weight functions are

$$\begin{aligned} w_{\{1,2,4\}}[x_1, x_2, x_3] &= \frac{1}{x_1 x_2 x_3}, \\ w_{\{1,3,4\}}[x_1, x_2, x_3] &= \frac{1}{x_1(1-x_1-x_2)x_3}, \\ w_{\{2,3,4\}}[x_1, x_2, x_3] &= \frac{1}{(1-x_1-x_2)x_2 x_3}, \\ w_{\{1,2,5\}}[x_1, x_2, x_3] &= \frac{1}{x_1 x_2(2-x_1-x_2-x_3)}, \\ w_{\{1,3,5\}}[x_1, x_2, x_3] &= \frac{1}{x_1(1-x_1-x_2)(2-x_1-x_2-x_3)}, \\ w_{\{2,3,5\}}[x_1, x_2, x_3] &= \frac{1}{(1-x_1-x_2)x_2(2-x_1-x_2-x_3)}. \end{aligned}$$

The key to generalizing the simple construction to the non-simple case is to observe the effect of slightly perturbing the entries of the matrix N . The half-spaces defined by the perturbed matrix N define a new simple polytope in which each non-simple vertex has split into a collection of simple vertices. For example, perturbing the half-spaces defining a square pyramid (non-simple) yields a triangular prism (simple). In particular, the vertex of the square pyramid (where four planes meet) splits into two vertices where three planes meet. Now, to construct a barycentric coordinate function for non-simple vertex v , we simply add the barycentric coordinate functions for its corresponding simple vertices. Given a non-simple vertex v_σ lying on k common faces (where $\sigma = \{1, \dots, k\}$), one suitable decomposition for v_σ is into the $k-2$ simple vertices $v_{\{1,j,j+1\}}$ where $2 \leq j \leq k-1$. For example, consider the square pyramid defined by the five half-spaces as show on the right of figure 2.

$$\begin{pmatrix} -1 & 0 & 0 \\ 0 & -1 & 0 \\ 1 & 1 & 0 \\ 0 & 0 & -1 \\ -1 & -1 & 1 \end{pmatrix} \begin{pmatrix} x_1 \\ x_2 \\ x_3 \end{pmatrix} \leq \begin{pmatrix} 0 \\ 0 \\ 1 \\ 0 \\ 0 \end{pmatrix}.$$

This square pyramid has five vertices that are indexed as

$$v_{\{1,4,2,5\}}, v_{\{1,3,4\}}, v_{\{2,3,4\}}, v_{\{1,3,5\}}, v_{\{2,3,5\}}$$

with their corresponding positions being

$$(0, 0, 0), (0, 1, 0), (1, 0, 0), (0, 1, 1), (1, 0, 1).$$

Since the vertex $v_{\{1,4,2,5\}}$ is non-simple, this vertex is decomposed into the union of two simple vertices $v_{\{1,2,4\}}$ and $v_{\{1,2,5\}}$.

$$\begin{aligned} w_{\{1,4,2,5\}}[x_1, x_2, x_3] &= \frac{x_1 + x_2}{x_1 x_2 (x_1 + x_2 - x_3) x_3}, \\ w_{\{1,3,4\}}[x_1, x_2, x_3] &= \frac{1}{x_1(1-x_1-x_2)x_3}, \\ w_{\{2,3,4\}}[x_1, x_2, x_3] &= \frac{1}{(1-x_1-x_2)x_2 x_3}, \\ w_{\{1,3,5\}}[x_1, x_2, x_3] &= \frac{1}{x_1(1-x_1-x_2)(x_1+x_2-x_3)}, \\ w_{\{2,3,5\}}[x_1, x_2, x_3] &= \frac{1}{(1-x_1-x_2)x_2(x_1+x_2-x_3)}. \end{aligned}$$

```
// Compute barycentric coordinates in 3D
sumW ← 0
for each v_σ (σ is a list of indices to faces ordered clockwise)
  // Assume (without loss of generality) that σ = {1..k}
  w_σ[x] ← 0 // initialization
  n_1[x] ← (v_σ - x) · N_1 // distance from x to face 1
  for j = 2..(k-1)
    // Compute volume V of normals N_1, N_j, N_{j+1}
    V ← |N_1 · (N_j × N_{j+1})|
    n_j[x] ← (v_σ - x) · N_j
    n_{j+1}[x] ← (v_σ - x) · N_{j+1}
    n_{1,j,j+1}[x] ← n_1[x] n_j[x] n_{j+1}[x] // form denominator
  w_σ[x] += V/n_{1,j,j+1}[x]
sumW += w_σ[x]
// Normalization of the coordinates
for each v_σ
  b_σ[x] = w_σ[x]/sumW
```

Figure 3: Barycentric coordinates on 3D polytopes

Of course, this construction seems to depend on the particular perturbation used in decomposing v . However, as shown in Warren [Warren 1996], this construction is independent of the particular perturbation chosen. The proof formalizes the perturbation argument by constructing the projective dual of P and then triangulating the facet that is dual to the non-simple vertex v . The simplices forming the triangulation of this facet are dual to a set of simple vertices all coincident with v . The proof then shows that the construction for barycentric coordinates is independent of any particular triangulation.

In terms of our previous example, this property means that using an alternative decomposition of $v_{\{1,4,2,5\}}$ into $v_{\{1,4,5\}}$ and $v_{\{2,4,5\}}$ yields the same weight function. In particular, the sums $w_{\{1,2,4\}}[x] + w_{\{1,2,5\}}[x]$ and $w_{\{1,4,5\}}[x] + w_{\{2,4,5\}}[x]$ are identical. This observation allows us to design a simple pseudo-code to efficiently compute barycentric coordinates for 3D convex polytopes, as given in Figure 3.

3 Barycentric coordinates for smooth convex sets

For a convex polytope P , barycentric coordinates blend values f_v assigned to the vertices of P to define a function $f[x]$ over all of P . In some applications, we would like to perform a similar blending for arbitrary convex shapes. In particular, given a function $f[t]$ defined on the boundary of P , ∂P , we desire a method for extending $f[t]$ to the interior of P that generalizes barycentric coordinates from the polytope case. In this section, we sketch such a construct and give more details in the case of $d=2$.

Given a d -dimensional convex set P whose boundary ∂P has a parameterization $p[t]$ (with $t \in \mathbb{R}^{d-1}$), a *barycentric coordinate* function $b[x, t]$ (with $x \in \mathbb{R}^d$) satisfies the three properties

$$\begin{aligned} b[x, t] &\geq 0 \quad \forall x \in P, \\ \int_{\partial P} b[x, t] dt &= 1 \quad \forall x, \\ \int_{\partial P} p[t] b[x, t] dt &= x \quad \forall x. \end{aligned} \tag{5}$$

Each of these three properties generalizes the corresponding property for the polytope case. Note that for strictly convex shapes (those whose supporting half-spaces contact the shape in a single

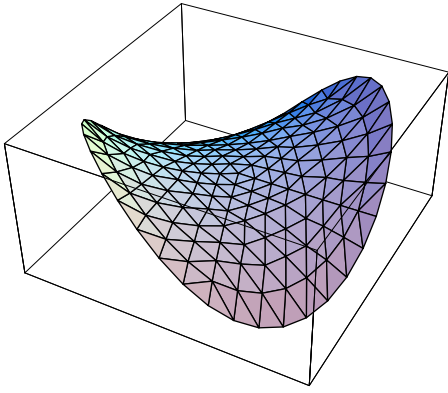


Figure 4: Barycentric interpolation of the function x_1x_2 on the unit circle: notice how the values blend on the interior of the circle in a smooth, natural manner.

point), the resulting barycentric coordinate functions degenerate to the Dirac delta function on the boundary of P ; that is

$$b[p[t_*], t] = \delta[t - t_*] \quad (6)$$

where $p[t_*]$ is point on ∂P and $\delta[t]$ is the Dirac delta function. For such shapes, the barycentric coordinate function can be used to perform boundary interpolation. In particular, given a function $f[t]$ that is defined on ∂P , we can compute an extension of f in the interior of P via the integral

$$\hat{f}[x] = \int_{\partial P} f[t]b[x, t]dt. \quad (7)$$

Note that due to equation 6, $\hat{f}[x]$ interpolates $f[t]$ on ∂P ; that is, $\hat{f}[p[t]] = f[t]$.

3.1 The general formula for smooth sets

One of the beautiful aspects of formula 3 is that it generalizes to smooth shapes in a very natural manner. The key observation is that the Gaussian curvature which is typically a continuous function on a sufficiently smooth convex polyhedra can be viewed as being zero on the faces and edges of the polyhedra and a collection of Dirac deltas at the vertices of P . Plugging these deltas in the continuous integral of equation 7 yields a discrete sum similar to equation 2. Given a parameterization $p[t]$ of ∂P , we consider the continuous weight function $w[x, t]$

$$w[x, t] = \frac{\kappa[t]\alpha[t]}{(\mathbf{v}[t] \cdot (p[t] - x))^d} \quad (8)$$

where $\kappa[t]$ is Gaussian curvature at $p[t]$, $\alpha[t]$ is the volume of the first fundamental form of $p[t]$ and $\mathbf{v}[t]$ is the unit normal to $p[t]$. Note the resulting weight function is independent of the choice of parameterization $p[t]$ due to inclusion of the factor of $\alpha[t]$. Next, we compare the numerator and denominator of equation 8 to the that of formula 3.

In the discrete case, the numerator $|\text{Det}[N_\sigma]|$ corresponds to the volume of parallelepiped spanned by the unit vectors N_j where $j \in \sigma$. If we normalize this expression by $\frac{1}{dt}$, this expression approximates the area of the patch spanned by the normals N_j on the Gauss sphere. In the continuous case, DoCarmo [DoCarmo 1976] defines the Gaussian curvature $\kappa[t]$ to be the limit of the area of the image of an infinitesimal patch dt on the Gaussian sphere divided by the area of the patch dt . Since $\alpha[t]$ corresponds to the area of this patch, the expression $\kappa[t]\alpha[t]$ corresponds to simply the infinitesimal area of patch on the Gauss sphere. For the denominator,

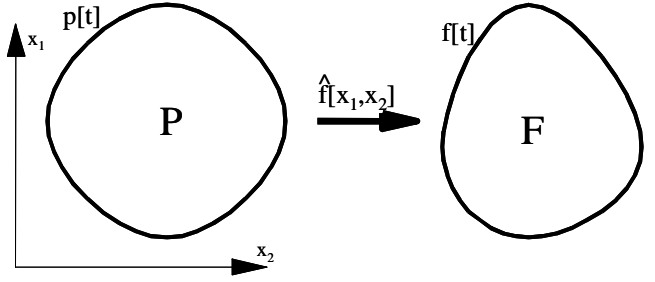


Figure 5: $\hat{f}[x_1, x_2]$ provides a map between $p[t]$ and $f[t]$. This map can be used to perform free-form deformations.

the d discrete normal vectors N_j converge to the continuous normal vector $\mathbf{v}[t]$.

To complete the construction, we define a barycentric coordinate function $b[x, t]$ associated with $w[x, t]$ to have the form

$$b[x, t] = \frac{w[x, t]}{\int_{\partial P} w[x, t]dt}. \quad (9)$$

After this normalization, these coordinate functions $b[x, t]$ are non-negative and sum to one.

3.2 A specialized 2D formula

We next consider an explicit construction for $w[x, t]$ in the case of 2D convex regions. Given a parameterization $p[t] = (p_1[t], p_2[t])$ for the closed convex curve ∂P , we recall that $\alpha[t]$ (the length of the first fundamental form) is the length of the tangent vector $(p'_1[t], p'_2[t])$, i.e;

$$\alpha[t] = (p'_1[t]^2 + p'_2[t]^2)^{\frac{1}{2}}.$$

Moreover, the curvature $\kappa[t]$ has the form

$$\kappa[t] = \frac{p'_1[t]p''_2[t] - p'_2[t]p''_1[t]}{\alpha[t]^3}$$

while the unit normal $\mathbf{v}[t]$ is the vector $\frac{1}{\alpha[t]}(-p'_2[t], p'_1[t])$. After simplification, the weight function $w[x, t]$ of equation 8 reduces to

$$w[x_1, x_2, t] = \frac{p'_1[t]p''_2[t] - p'_2[t]p''_1[t]}{((-p'_2[t], p'_1[t]) \cdot (x_1 - p_1[t], x_2 - p_2[t]))^2}. \quad (10)$$

The resulting function for $b[x_1, x_2, t]$ is non-negative and has unit integral by construction. Furthermore, the appendix contains a proof of linear precision that verifies that equation 10 yields a basis function $b[x_1, x_2, t]$ that satisfies equation 5.

To illustrate this formula, consider the unit disk whose boundary is the unit circle with parameterization $(x_1, x_2) = (\text{Cos}[t], \text{Sin}[t])$. By construction, the weight function $w[x_1, x_2, t]$ has the form

$$w[x_1, x_2, t] = \frac{1}{(x_1 \text{Cos}[t] + x_2 \text{Sin}[t] - 1)^2}.$$

The corresponding barycentric coordinate function $b[x_1, x_2, t]$ has the form

$$b[x_1, x_2, t] = \frac{(1 - x_1^2 - x_2^2)^{\frac{3}{2}}}{2\pi(x_1 \text{Cos}[t] + x_2 \text{Sin}[t] - 1)^2}.$$

To construct a function $\hat{f}[x_1, x_2]$ that interpolates the function x_1x_2 on the unit circle, we must build a function $f[t]$ parameterized over the boundary that interpolates x_1x_2 . Notice that $f[t] =$

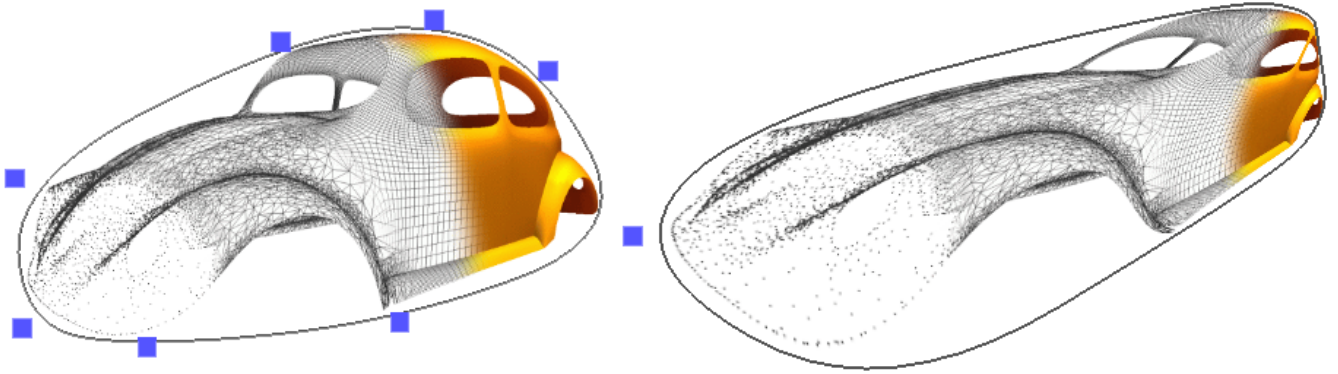


Figure 6: Car before deformation and bounding quadratic B-spline curve defining $p[t]$ (left). Deformed car generated by altering the control points with bounding curve $f[t]$ (right).

$\text{Cos}[t]\text{Sin}[t]$ since $(x_1, x_2) = (\text{Cos}[t], \text{Sin}[t])$. Now equation 7 can be computed analytically and has the form

$$\hat{f}[x_1, x_2] = \frac{x_1 x_2 \left(-2 + 3x_1^2 + 3x_2^2 + 2(1 - x_1^2 - x_2^2)^{\frac{3}{2}} \right)}{(x_1^2 + x_2^2)^2}.$$

Figure 4 shows a plot of this function restricted to the unit circle. Observe that the function $\hat{f}[x_1, x_2]$ interpolates the function $x_1 x_2$ on the unit circle while blending these values on the interior of the circle in a natural manner.

3.3 An application to freeform deformations

Continuous barycentric coordinates can be used to perform freeform deformations on images as well. Given a convex region P bounded by a smooth curve $p[t]$, we wish to deform P into another region F bounded by the curve $f[t]$ (see figure 5). The deformation $\hat{f}[x_1, x_2]$ is a vector-valued function that smoothly maps points in P to points in F with the property that points on $p[t]$ will map to points on $f[t]$, that is, $\hat{f}[p[t]] = f[t]$ and the map will be smooth on the interior of the regions.

In our example, we define P and F as the regions bounded by closed quadratic B-splines $p[t]$ and $f[t]$ having k control points on the periodic interval $0 \leq t \leq k$. Though B-splines are only piecewise polynomial, equation 7 still applies. In fact, any B-spline curve can be represented as a piecewise polynomial function of the form

$$\begin{aligned} p[t] &= p_i[t - i], \\ f[t] &= f_i[t - i], \quad i \leq t \leq i + 1 \end{aligned}$$

where $p_i[t]$, $f_i[t]$ are the i^{th} polynomial functions comprising the respective B-splines.

To compute equation 7 we need to construct $w[x_1, x_2, t]$, which is also a piecewise function, and has the form

$$w[x_1, x_2, t] = w_i[x_1, x_2, t - i], \quad i \leq t \leq i + 1$$

where $w_i[x_1, x_2, t]$ is formed using equation 10 for the function $p_i[t]$. With this result we can calculate the normalization factor in equation 9 as

$$\int_{\partial P} w[x_1, x_2, t] dt = \sum_{i=0}^{k-1} \int_0^1 w_i[x_1, x_2, t] dt.$$

Now we compute $\hat{f}[x_1, x_2]$ using equation 7 as a piecewise integral that has the form

$$\begin{aligned} \hat{f}[x_1, x_2] &= \frac{1}{\int_{\partial P} w[x_1, x_2, t] dt} \int_{\partial P} f[t] w[x_1, x_2, t] dt \\ &= \frac{1}{\int_{\partial P} w[x_1, x_2, t] dt} \sum_{i=0}^{k-1} \int_0^1 f_i[t] w_i[x_1, x_2, t] dt. \end{aligned}$$

We can explicitly calculate the integrals above, using a symbolic software package such as *Mathematica*, to obtain a closed form solution in terms of (x_1, x_2) and the control points of the B-splines forming $p[t]$ and $f[t]$. Though each $w_i[x_1, x_2, t]$ is a rational polynomial function, the resulting $\hat{f}[x_1, x_2]$ is more complicated and is in terms of functions such as *Arctan*. However, the function is still fast to evaluate (since no integrals need be computed) and the image deformation can be recomputed in realtime.

The user performs image deformation by first placing the control points of the curve $p[t]$ about the convex area that they wish to deform (see figure 6, left). Once the user is satisfied, the control points are duplicated to form the curve $f[t]$. The user then drags on the control points of $f[t]$ to generate the desired deformation. Due to the fact that barycentric coordinates interpolate the boundary (as shown in equation 6), the deformed image will follow the boundary of $f[t]$. Figure 6 (right) shows an example deformation of the car from the left portion of the figure. The entire application and source for performing these deformations can be downloaded from <http://www.cs.rice.edu/~sschaefe/barywhite.zip>.

4 Conclusion

In this paper we have provided an explicit construction for barycentric coordinates over polytopes that is valid in arbitrary dimensions and contains all of the desirable qualities described in section 1.1. After demonstrating several example constructions and providing pseudo-code for the 3D case, we extended barycentric coordinates to smooth convex functions. Finally, we showed that barycentric coordinates could be used for image deformation as well.

In future work, we plan on giving a proof of linear precision for the barycentric coordinates for smooth convex sets whose dimension is greater than two, and showing how our barycentric coordinates can be extended to non-convex polytopes using geometric inversion.

References

- DOCARMO, M. 1976. *Differential geometry of curves and surfaces*. Prentice-Hall.
- ECK, M., DE ROSE, T., DUCHAMP, T., HOPPE, H., LOUNSBERY, M., AND STUETZLE, W. 1995. Interactive Multiresolution Surface Viewing. In *ACM Siggraph'95 Conference*, 91–98.
- FLOATER, M., HORMANN, K., AND KÓ S, G. 2003. A general construction of barycentric coordinates over convex polygons. *Preprint*.

- FLOATER, M. S. 1997. Parametrization and smooth approximation of surface triangulations. *CAGD 14*, 3, 231–250.
- FLOATER, M. S. 1998. Parametric Tilings and Scattered Data Approximation. *International Journal of Shape Modeling 4*, 165–182.
- FLOATER, M. 2002. Mean Value Coordinates. *Preprint*.
- GOTSMAN, C., AND SURAHHSKY, V. 2001. Guaranteed Intersection-free Polygon Morphing. *Computer and Graphics 25*, 1, 67–75.
- KURIYAMA, S. 1993. Surface Generation from an Irregular Network of Parametric Curves. *Modeling in Computer Graphics, IFIP Series on Computer Graphics*, 256–274.
- LODHA, S. 1993. Filling N-sided Holes. *Modeling in Computer Graphics, IFIP Series on Computer Graphics*, 319–345.
- LOOP, C., AND DEROSE, T. 1989. A multisided generalization of Bézier surfaces. *ACM Transactions on Graphics 8*, 204–234.
- MEYER, M., LEE, H., BARR, A. H., AND DESBRUN, M. 2002. Generalized Barycentric Coordinates for Irregular Polygons. *Journal of Graphics Tools* (Nov.).
- PINKALL, U., AND POLTHIER, K. 1993. Computing Discrete Minimal Surfaces and Their Conjugates. *Experimental Math. 2*, 15–36.
- SIBSON, R. 1981. A brief description of natural neighbor interpolation. In *Interpreting Multivariate Data*, V. Barnett, Ed. John Wiley & Sons, 21–36.
- WACHPRESS, E. 1975. A Rational Finite Element Basis. *Manuscript*.
- WARREN, J. 1996. Barycentric Coordinates for Convex Polytopes. *Advances in Computational Mathematics 6*, 97–108.
- WARREN, J. 2002. On the uniqueness of barycentric coordinates. To appear in the Proceedings of the Vilnius Workshop on Algebraic Geometry and Geometric Modeling.

Appendix A

As observed in the paper, proving that the coordinate functions $b_\sigma[x]$ have linear precision reduces to showing that equation 4 holds; that is the weight functions $w_\sigma[x]$ satisfy

$$\sum_{v_\sigma \in P} (v_\sigma - x) w_\sigma[x] = 0.$$

To this end, we observe that at a vertex $v_\sigma \in P$, the following vector relationship holds

$$\frac{c_\sigma - N_\sigma x}{n_\sigma[x]} = \sum_{j=1}^d \frac{e_j}{n_{\sigma-j}[x]}$$

where e_j is the i -th basis vector in d dimensions. ($\sigma - j$ denotes the set σ with index j deleted.) Multiplying the numerator of both sides of this equation by N_σ^{-1} , the resulting equation has the form

$$\frac{v_\sigma - x}{n_\sigma[x]} = \sum_{j \in \sigma} \frac{N_\sigma^{-1} e_j}{n_{\sigma-j}[x]} \quad (11)$$

where $v_\sigma = N_\sigma^{-1} c_\sigma$. Now, we recall that the j -th column of N_σ^{-1} corresponds to the cross product of the $d - 1$ rows of $N_{\sigma-j}$ divided by the determinant of N_σ . Applying this observation and multiplying both sides of equation 11 by $\text{Det}[N_\sigma]$ yields that

$$(v_\sigma - x) \frac{\text{Det}[N_\sigma]}{n_\sigma[x]} = \sum_{j \in \sigma} \frac{\text{Cross}[N_{\sigma-j}]}{n_{\sigma-j}[x]} \quad (12)$$

Note that each of the cross products in equation 12 corresponds to a vector lying parallel to an edge of P incident to v_σ . Taking the sum of both sides of equation 12 over all $v_\sigma \in P$ yields

$$\sum_{v_\sigma \in P} (v_\sigma - x) \frac{\text{Det}[N_\sigma]}{n_\sigma[x]} = \sum_{v_\sigma \in P} \sum_{j \in \sigma} \frac{\text{Cross}[N_{\sigma-j}]}{n_{\sigma-j}[x]}. \quad (13)$$

Now, we assume (without loss of generality) that the indices in σ are ordered such that the determinant of N_σ is always positive. Since each edge of P is shared by two vertices of P , the cross product on the right-hand side of equation 13 appears twice in the double summation, once for each possible orientation of the edge. Since these vector then cancel, the left hand side of equation 13 is identically zero. Observing that $\frac{\text{Det}[N_\sigma]}{n_\sigma[x]}$ is exactly the weight function $w_\sigma[x]$ defined by formula 3 completes the proof.

Appendix B

We now prove that the specialized 2D coordinate function $b[x, t]$ provided in section 3.2 satisfies the properties that define continuous barycentric coordinate functions from equation 5. The first, two properties (non-negativity and unit integral) are verified by construction of $b[x, t]$. Therefore, we must show that $b[x, t]$ has linear precision, which is stated as

$$x = \int_{\partial P} p[t] b[x, t] dt.$$

Substituting the definition of $b[x, t]$ from equation 9 yields

$$x \int_{\partial P} w[x, t] dt = \int_{\partial P} p[t] w[x, t] dt.$$

Rewriting this equation as a single integral, we obtain

$$\int_{\partial P} (x - p[t]) w[x, t] dt = 0.$$

Substitution of the definition of $w[x, t]$ from equation 10 creates the specialized two-dimensional equation

$$\int_{\partial P} \frac{(x_1 - p_1[t], x_2 - p_2[t])(p_1'[t] p_2''[t] - p_2'[t] p_1''[t])}{((-p_2'[t], p_1'[t]) \cdot (x_1 - p_1[t], x_2 - p_2[t]))^2} = 0.$$

Integrating the indefinite integral yields the function

$$\frac{(p_1'[t], p_2'[t])}{(-p_2'[t], p_1'[t]) \cdot (x_1 - p_1[t], x_2 - p_2[t])}.$$

Since the integral is evaluated over a closed path, the definite integral is zero. Therefore, the specialized 2D coordinate function $b[x, t]$ satisfies equation 5.